

UNIVERSITAT DE BARCELONA

FACULTAT DE FÍSICA

Màster en Biofísica

**Resonant spike propagation in coupled neurons
with subthreshold activity**

Treball final del Màster en Biofísica 2006/07:

Belén Sancristóbal Alonso

Tutor: José María Sancho and Jordi Garcia-Ojalvo

Contents

1	Introduction	1
2	FitzHugh-Nagumo model	2
2.1	Stability analysis	5
2.2	Noise and spectral analysis	8
3	Coupling neurons	10
3.1	Electrical coupling	10
3.2	Chemical coupling	11
4	Modified FitzHugh-Nagumo model	11
4.1	Stability analysis	12
4.2	Time scale of subthreshold oscillations	13
5	Spike propagation in coupled neurons	15
5.1	Electrical coupling: resynchronization <i>versus</i> damping	15
5.2	Chemical coupling: modulating spike excitation <i>via</i> subthreshold oscillations	18
5.3	Effect of delay in synaptic transmission	19
6	Conclusions	22

Abstract

Chemical coupling between neurons is only active when the presynaptic neuron is firing, and thus it does not allow for the propagation of subthreshold activity. Electrical coupling via gap junctions, on the other hand, is also ubiquitous and, due to its diffusive nature, transmits both subthreshold and suprathreshold activity between neurons. We study theoretically the propagation of spikes between two neurons that exhibit subthreshold oscillations, and which are coupled via both chemical synapses and gap junctions. Due to the electrical coupling, the periodic subthreshold activity is synchronized in the two neurons, and affects propagation of spikes in such a way that for certain values of the delay in the synaptic coupling, propagation is not possible. This effect could provide a mechanism for the modulation of information transmission in neuronal networks.

1 Introduction

Information transmission in the form of spike propagation plays a vital role in the functioning of the nervous system [1]. The excitable nature of the neuronal response to perturbations allows for the untarnished propagation of action potentials along chains of neurons, coupled chemically to one another

via unidirectional synaptic connections. But chemical synapses are only activated when the presynaptic neuron undergoes an action potential, which elicits a constant-shaped postsynaptic potential (PSP) at the receiving neuron. Therefore, the only kind of information that is transmitted between neurons due to synaptic coupling is the timing at which spikes occur. However, an increasing amount of evidence shows that subthreshold oscillations constitute an important part of the dynamical activity of neurons [2], and thus the question arises as to what is the functional role of subthreshold activity. Here we study a potential effect of subthreshold oscillations in modulating the propagation of spikes along a chain of neurons.

Indeed, since successful propagation of a spike requires that the postsynaptic neuron overcomes its excitation threshold upon receipt of the synaptic current, the state of the postsynaptic neuron at the time at which it receives the synaptic pulse determines strongly whether a postsynaptic spike will be produced. This is specially relevant for neurons with subthreshold oscillations: if the pulse arrives to the neuron at around a minimum of a subthreshold oscillation, the effective distance to the excitation threshold will be large, and one could expect that producing a spike would become more difficult. Oppositely, when the pulse arrives near a maximum of a subthreshold oscillation, excitation should be easier. Consequently, one would expect that the propagation efficiency of a neuronal system would depend on the relationship between the period of the subthreshold oscillations and the delay incurred in the propagation due to the time required by the synaptic mechanism to operate. A coherent modulation of the propagation efficiency along a chain of neurons should be expected when the subthreshold activity between all neurons in the chain is synchronized. This can be accomplished by means of diffusive coupling due to gap junctions, which is also ubiquitous in neural tissue [1]. In this work, we examine this possibility by studying the propagation of a spike train between two neurons, coupled via both synapses (with a delay) and gap junctions (instantaneously). Our results show that propagation appears resonantly, only for certain values of the synaptic delay such that the presynaptic pulse arrives at the receiving neuron at the right time to elicit a spike in it.

2 FitzHugh-Nagumo model

A classical model for the dynamics of a cell membrane potential V is one that considers a cell membrane as a capacitor C_m and a resistor R in parallel.

We can then establish a differential equation for the time evolution of V as

$$C_m \frac{dV}{dt} = -\frac{V - E_{eq}}{R} + I \quad (1)$$

where E_{eq} is the rest potential or Nernst equilibrium potential at which the net cross-membrane current is zero and I is the total current. The current across the inner and outer surfaces of the cell membrane involves mainly four ionic species: sodium (Na^+), potassium (K^+), calcium (Ca^{2+}) and chloride (Cl^-). The concentration of each ion inside the cell is different from the concentration on the extracellular medium which is rich on Na^+ and Cl^- for instance. Due to this difference in the ionic concentrations, electrochemical gradients produce chemical flows through the existing channels along the membrane, which cause changes in the membrane potential. If there are no other additional currents then $I = 0$ because the concentration gradient and the electric potential gradient are balanced and equilibrium is achieved.

However an active transport makes impossible to achieve a symmetry between the inner and outer concentrations. The flow produced by the ionic pumps like the Na^+-K^+ pump pumps out three Na^+ ions for every two K^+ ions pumped in. The concentration gradients are also maintained due to the negatively charged molecules inside the cell that attract more K^+ into the cell and repel more Cl^- out of the cell.

In the model of Hodgkin and Huxley (1952) the term $1/R$ of equation (1) depends on the ionic flows which are in turn controlled by gating particles (gates), see Fig. 1. These particles can open and close the channels and are sensitive to the membrane potential. The model equation, which only takes into account three major currents, is then:

$$C_m \frac{dV}{dt} = -g_K n^4 (V - E_K) - g_{Na} m^3 h (V - E_{Na}) - g_L (V - E_L) + I \quad (2)$$

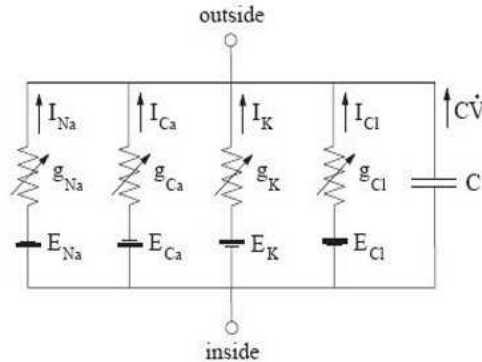


Figure 1: Equivalent circuit representation of a patch of cell membrane. This figure is directly taken from [4].

where the subscript L corresponds to the leak current, which is carried mostly by Cl^- ions. The terms g_K , g_{Na} and g_L are the maximal conduc-

tances (inverse of the maximal resistances), for which typical values are $g_K = 36mS/cm^2$, $g_{Na} = 120mS/cm^2$ and $g_L = 0.3mS/cm^2$. The variables m and h determine the probability of the activation and inactivation, respectively, of the Na^+ current. The variable n determines the probability of the activation of the K^+ current. The combination of these three variables gives the average proportion of channels in the open state. The term n^4 is then referred to the four activation gates of the voltage-gated persistent K^+ current and m^3h is referred to the three activation gates and one inactivation gate of voltage-gated transient Na^+ current. The dynamics of these variables are assumed to follow first order kinetics:

$$\tau_w \frac{dw}{dt} = w_\infty(V) - w, \quad w = n, h, m \quad (3)$$

where $\tau_w(V)$ and $w_\infty(V)$ are the time constant and rate constant, respectively, and are empirical functions. For a fixed potential V , the variable w approaches the value $w_\infty(V)$ with a time constant $\tau_w(V)$.

The equations (2) and (3) represent a four-dimensional dynamical system known as the Hodgkin-Huxley model. The time-dependent evolution of conductances allows a neuron to produce pulses of voltage called *action potentials* or *spikes*. Other neuronal models have additional currents with other activation and desactivation dynamics.

In the 1950's FitzHugh reduced the Hodgkin-Huxley model to a two variable model. He observed that the gating variables n and h have slow kinetics relative to m that can be then treated as an instantaneous variable which rapidly takes its steady-state value $m_\infty(V)$. Another important fact is that the time constants $\tau_n(V)$ and $\tau_h(V)$ are very similar independently of the potential V . Even the functions $n_\infty(V)$ and $1 - h_\infty(V)$ are also very similar (Fig. 2). We are then allowed to use an effective variable w for n and $1-h$.

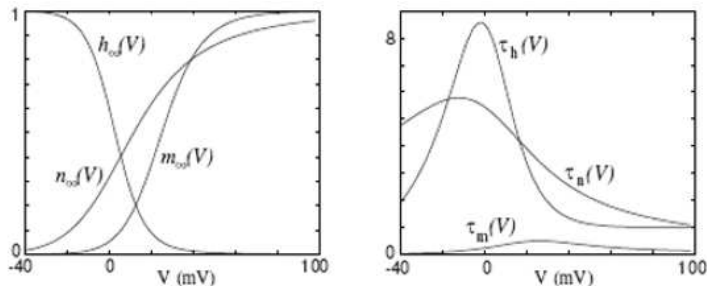


Figure 2: Steady-state (in)activation functions (left) and voltage-dependent time constants (right) in the Hodgkin-Huxley model. This figure is directly taken from [4].

Once we applied these simplifications to equation (2) we get:

$$C_m \frac{dV}{dt} = -g_K \left(\frac{w}{a}\right)^4 (V - E_K) - g_{Na} (m_\infty(V))^3 (b - w)(V - E_{Na}) - g_L(V - E_L) + I \quad (4)$$

where for generality we have written $w = b - h = an$. Equation (4) can be further simplified by writing

$$\frac{dV}{dt} = \frac{1}{\tau} [F(V, w) + RI] \quad (5)$$

where $\tau = RC_m$ and $R = g_L^{-1}$. Finally equation (3) can be rewritten for w , leading to a single effective equation

$$\frac{dw}{dt} = \frac{1}{\tau_w} G(V, w) \quad (6)$$

FitzHugh and Nagumo build up a system of two equations like (5) and (6) replacing the functions F and G by

$$F(V, w) = V - V^3 - w \quad (7)$$

$$G(V, w) = b + \gamma V - w \quad (8)$$

in order to reproduce qualitatively the behavior of a neuron.

2.1 Stability analysis

The FitzHugh-Nagumo equations are a model for a nonlinear dynamical system, like neurons, which can be studied from its phase portrait. For $I = 0$ we can look at different regimes by varying the parameters of the model which in turn determine the intersection point between the nullclines and the stability of that point.

The nullclines are the curves where $\frac{dV}{dt} = 0$ or $\frac{dw}{dt} = 0$ and it is where the change of sign of the derivatives takes place, i.e. the functions $V(t)$ and $w(t)$ go from increasing to decreasing or viceversa. The intersection between the two nullclines corresponds to an *equilibrium point* (also named *fixed point*) that can be stable or unstable. The stability of the equilibrium point can be analyzed by looking at the behavior of a trajectory starting close to it. In other words, we can linearize the nonlinear functions F and G near the equilibrium (V_o, w_o) building up the Jacobian matrix of the system J as

$$\frac{d}{dt} \begin{pmatrix} \bar{V} \\ \bar{w} \end{pmatrix} = \begin{pmatrix} \frac{1}{\tau} \partial F / \partial V & \frac{1}{\tau} \partial F / \partial w \\ \frac{1}{\tau_w} \partial G / \partial V & \frac{1}{\tau_w} \partial G / \partial w \end{pmatrix}_{(V_o, w_o)} \begin{pmatrix} \bar{V} \\ \bar{w} \end{pmatrix} \quad (9)$$

where $\bar{V} = V - V_o$ and $\bar{w} = w - w_o$ are the deviations from the equilibrium. Looking at the eigenvalues and the eigenvectors of this matrix

$$J\vec{v} = \lambda\vec{v} \quad (10)$$

helps us to write a general solution for the linear system in the form

$$\begin{pmatrix} \bar{V}(t) \\ \bar{w}(t) \end{pmatrix} = c_1 e^{\lambda_1 t} v_1 + c_2 e^{\lambda_2 t} v_2 \quad (11)$$

with

$$\lambda_{1,2} = \frac{\tau \pm \sqrt{\tau^2 - 4\Delta}}{2} \quad (12)$$

where λ_1 and λ_2 are the eigenvalues of the eigenvectors v_1 and v_2 , respectively, c_1 and c_2 are constants, and τ and Δ are the trace and the determinant of the Jacobian matrix, respectively. Knowing the values of τ and Δ can tell us the nature of the eigenvalues and thus the way the trajectories behave around the fixed point according to equation (11) and (12). If both eigenvalues have negative real part the phase plane trajectory can move back to the fixed point oscillating around it (*stable*, complex eigenvalues) or approaching it asymptotically (*asymptotically stable*, real eigenvalues). If at least one eigenvalue has positive real part small perturbations are amplified and the system escapes the fixed point (*unstable*). Thus the necessary and sufficient condition for stability is $\Delta \geq 0$ and $\tau < 0$. This allows us to classify the equilibrium points besides their stability: if the eigenvalues are real and of the same sign we talk about *nodes*, if they have opposite signs they are called *saddles*, and if they are complex they are *foci*.

In dimensionless form our system of equations reads:

$$\epsilon \frac{dV}{dt} = V - V^3 - w, \quad (13)$$

$$\frac{dw}{dt} = b + \gamma V - w \quad (14)$$

where $\epsilon = \frac{\tau}{\tau_w}$. Setting $\gamma = 1.5$ we get two cases, see Fig. 3, within the excitable regime [5]: monotonic relaxation (e.g. point B, $\epsilon = 0.001$, $b = 0.6$) and damped oscillations (e.g. point A, $\epsilon = 0.05$, $b = 0.5$) of membrane potential that take the neuron to the resting state. These two types of neurons are called *nonresonant neurons* and *resonant neurons* respectively and their time series and phase portrait are represented in Figs. 4 and 5 respectively. In each phase portrait the nullclines and a typical trajectory

are represented.

Tuning the parameter b changes the coordinates of the fixed point.

$$b = -V_o^3 - \frac{1}{2}V_o \quad (15)$$

For the specific value $b = \frac{5}{2} \left(\frac{1}{3}\right)^{3/2}$ the equilibrium point is exactly at the minimum of the V -nullcline. On the other hand, the parameter ϵ modifies the stability of the fixed point by changing the sign of the radicand of equation (12).

$$\tau = \frac{1}{\epsilon} (1 - 3V_o^2) - 1 \quad (16)$$

$$\Delta = \frac{1}{\epsilon} \left(\frac{1}{2} + 3V_o^2 \right) \quad (17)$$

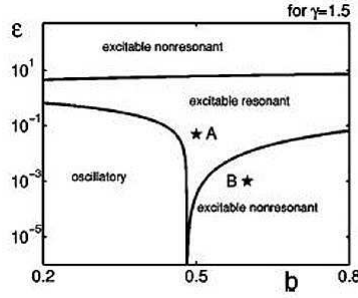


Figure 3: Stability diagram of the FitzHugh-Nagumo model in parameter space (ϵ, b) for constant $\gamma = 1.5$. Points A and B denote parameter sets used to model resonant and nonresonant neurons respectively. This figure is directly taken from [5].

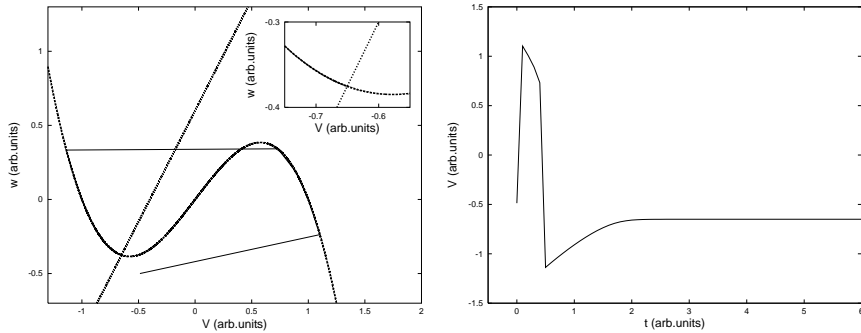


Figure 4: Phase portrait for a nonresonant neuron (left) and its potential time evolution (right).

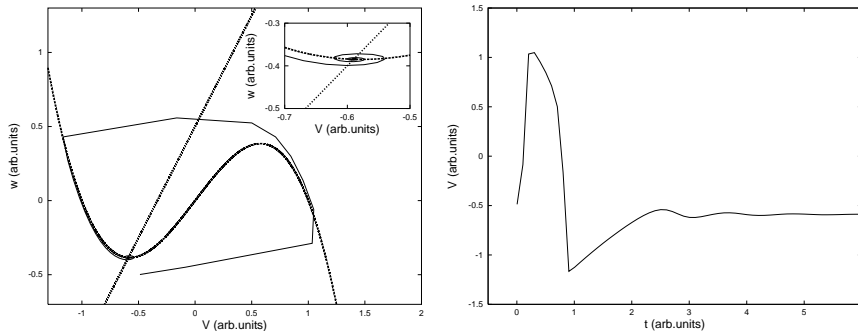


Figure 5: Phase portrait for a resonant neuron (left) and its potential time evolution (right).

In Fig. 4 we have a stable node with a trajectory that converges to the equilibrium point and in Fig. 5 we have a stable focus having a rotation around the equilibrium point.

2.2 Noise and spectral analysis

We can go further by considering the influence of the environment of a neuron, which receives continuously multiple signals from its neighbours. We can model this situation by adding to the equations a white Gaussian noise term, $\xi(t)$, with zero mean and correlation $\langle \xi(t)\xi(t') \rangle = 2D\delta(t - t')$. In the absence of external current the stochastic differential equation reads

$$\epsilon \frac{dV}{dt} = V - V^3 - w, \quad (18)$$

$$\frac{dw}{dt} = b + \gamma V - w + \sqrt{2D}\xi(t) \quad (19)$$

A neuron receives an irregular spike sequence due to the neural network activity. This noise can induce going from the resting state to excited state. In what follows we will focus on the resonant neuron type because we are interested in different phenomena related to the subthreshold oscillations, i.e. the propagation of the spikes. In Fig. 6 we can see the bursting effect produced by a stochastic current with amplitude $D = 0.0004$ where the subthreshold oscillations are disrupted by the noise.

In the presence of noise the resonant neuron shows an irregular pattern of spike generation that has in fact its own oscillatory frequencies. By looking at the power spectral density of the neuron it is easy to see that there are specific frequencies that control its behavior at different values of the noise intensity, D . The spectra of Fig. 7 were numerically obtained from a sample of 2^{15} points of the time series $V(t)$, with a sample interval 0.1 and averaged over 120 different realizations following [5]. The spectra are not normalized.

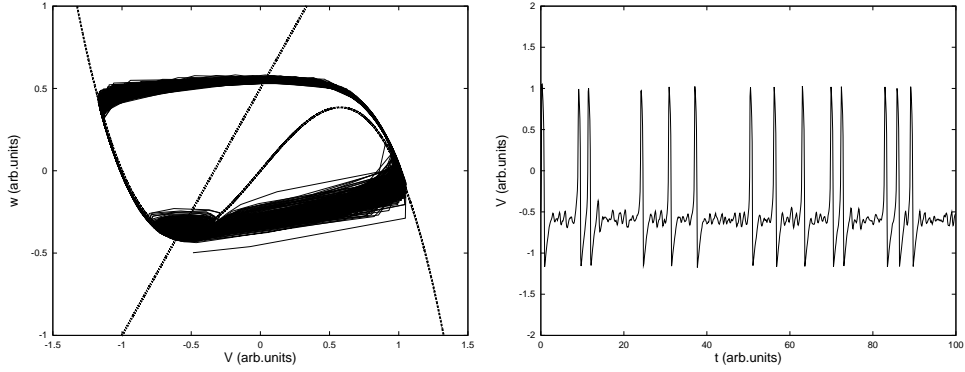


Figure 6: Phase portrait for a resonant neuron (left) and its potential time evolution (right) for $D=0.0004$.

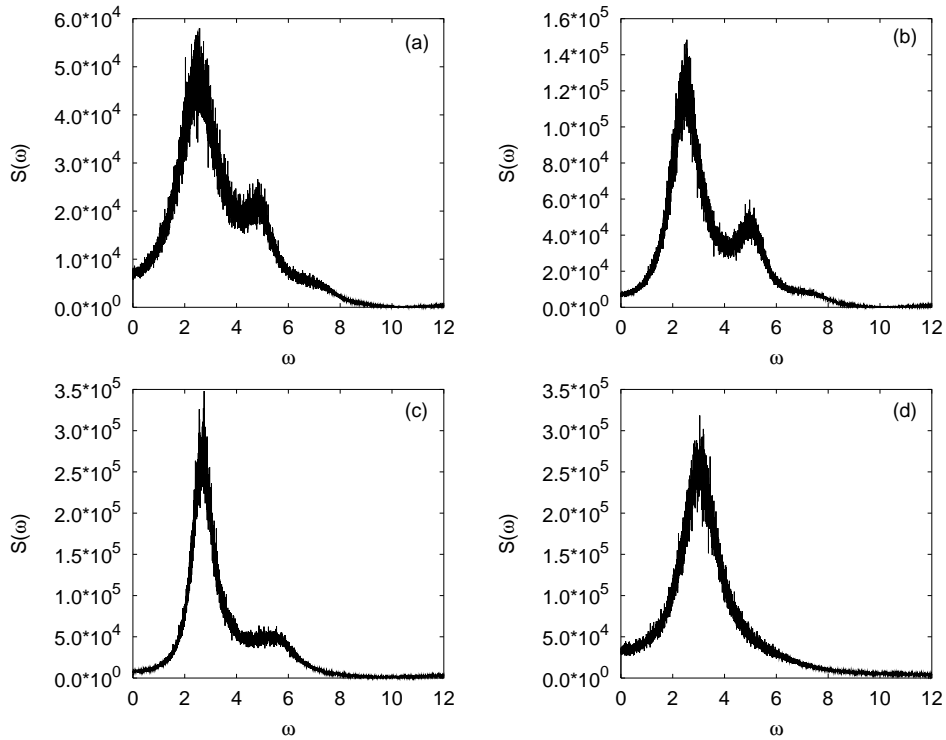


Figure 7: Spectra of the stochastic FitzHugh-Nagumo model in the resonant regime for increasing noise intensities: (a) $D = 0.0004$, (b) $D = 0.001$, (c) $D = 0.01$, (d) $D = 0.1$.

All the spectra of Fig. 7 show a main peak at a frequency that slightly increases at high levels of noise. This frequency corresponds to the mean firing frequency which is equal to $2\pi/T_1$, where T_1 is the time interval between the beginning of a spike and the first maximum of the subthreshold oscillations. The lower peak corresponds to the time interval between the beginning of a spike and the second maximum of the subthreshold oscillations and disappears at high levels of noise [Fig. 7 (d)]. Thus the difference between both frequencies corresponds to the frequency of the subthreshold oscillations [5]. If the environment is very noisy the subthreshold activity is significantly altered and the periodic subthreshold oscillations disappear.

3 Coupling neurons

When we study a network of neurons we must take into account their coupling in order to see how the information is transmitted through the network. As mentioned above, there are regions between neurons named *synapses* where the sending neuron is connected to the receiving neuron (see Fig. 8). There exist two types of synapses: electrical and chemical.

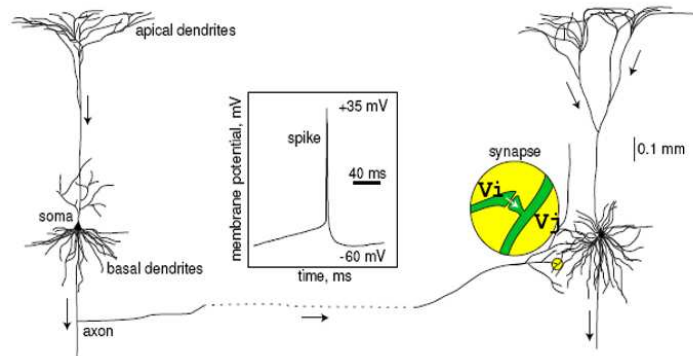


Figure 8: Two interconnected cortical pyramidal neurons (hand drawing) and *in vitro* recorded spike. V_i and V_j represent the voltage variable of the presynaptic and postsynaptic neuron respectively. This figure is directly taken from [4].

3.1 Electrical coupling

Electrical synapses are called *gap junctions*, and are connections between the cytoplasm of two cells where different ions flow. The electrical current produced is a way of fast transmission that changes the membrane potential of both neurons. The electrical coupling depends on the membrane potential difference between the two neurons:

$$I_i^{elec} = g^{elec} (V_i - V_j) \quad (20)$$

where $i = 1, 2$ index the neurons and g^{elec} is the effective conductance of the gap junction. This term will be added to the voltage variable equation (5) of each neuron.

3.2 Chemical coupling

The current in the presynaptic neuron leads to a release of messenger particles from the presynaptic neuron, known as neurotransmitters. The neurotransmitters are molecules that bind to protein receptors found in the postsynaptic neuron membrane. The chemical current is unidirectional and can be modeled by the following current term [6]:

$$I_i^{chem} = g^{chem} r_j (V_i - E_s) \quad (21)$$

where g^{chem} is the conductance of the synaptic channel, r_j represents the fraction of bound receptors of the postsynaptic neuron i (which depends on the firing times of the presynaptic neuron j), and E_s is fixed to a particular value in order to make the synapse excitatory (in the FitzHugh-Nagumo model presented up till now $E_s = 0$). The fraction of bound receptors has the following dynamical behavior [7]

$$\dot{r}_j = \alpha C_j (1 - r_j) - \beta r_j \quad (22)$$

where α and β are rise and decay time constants, respectively, and

$$C_j = C_{max} \theta((T_o^j - \tau) + \tau_{syn} - t) \theta(t - (T_o^j - \tau)) \quad (23)$$

is the concentration of neurotransmitters released into the synaptic cleft. T_o^j is the time at which the presynaptic neuron j fires, which happens whenever the presynaptic membrane potential exceeds a predetermined threshold value E_s . The time during which the synaptic connection is active is given by τ_{syn} . We add a time delay τ into the chemical current known as the synaptic delay to model a more realistic situation in which some time is needed for the neurotransmitter to be released, diffuse across the cleft, and bind to the receptor. The term I_i^{chem} only affects the postsynaptic neuron i and is also added to the voltage variable equation (5).

4 Modified FitzHugh-Nagumo model

The resonant neuron obtained from the previous FitzHugh-Nagumo model shows too weak subthreshold oscillations that quickly relax (Fig. 5). In order

to obtain relatively strong subthreshold oscillations we modify this model [8]. In dimensionless form, the modified model reads

$$\epsilon \dot{u} = u(u - a)(1 - u) - v, \quad (24)$$

$$\dot{v} = g(u - b) \quad (25)$$

where u is the voltage variable, and v is the recovery variable, which represents the effective membrane conductivity. The parameter ϵ is the ratio between the characteristic times of u and v . The u -nullcline still has the shape of a cubic function which can be obtained from the V -nullcline of equation (7) by a linear change of variables. Equation (8) is replaced by a monotonically increasing function,

$$g(x) = k_1 x^2 + k_2 \left(1 - \exp \left[-\frac{x}{k_2} \right] \right) \quad (26)$$

where k_1 and k_2 control the value of $\frac{dv}{dt}$ and, consequently, the time spent by a trajectory in the domain of $\frac{du}{dt} = 0$. The w -nullcline is just the straight line $u = b$. The equilibrium point is then $u_o = b$ and $v_o = b(b - a)(1 - b)$.

4.1 Stability analysis

The choice of the parameters ϵ , a and b depends on the regime considered. As mentioned above we are looking for a neuron having both oscillatory and excitatory properties. When the resting state undergoes a transition from stable (eigenvalues with negative real parts, Fig. 5) to unstable focus (eigenvalues with positive real parts) giving rise to a small-amplitude limit cycle attractor, we talk about a supercritical Andronov-Hopf bifurcation. We then lose stability of the fixed point but gain stable oscillations. Near the supercritical Andronov-Hopf bifurcation the FitzHugh-Nagumo model generates low amplitude quasiharmonic oscillations remaining excitable. From the local linear analysis we can see which role the parameters play. The mechanism followed is the same that took us to equation (11). For the system (24), (25) we build up the determinant and the trace of the Jacobian matrix at the fixed point:

$$\Delta = 1/\epsilon, \quad (27)$$

$$\tau = \frac{1}{\epsilon}(-b^3 + (1 - a)b^2 - ab) \quad (28)$$

Their sign depends on a and b . We will fix the parameter values $\epsilon = 0.005$ and $a = 0.9$ and vary b .

There is an important feature of τ . As the equation (25) does not depend on v , the trace of our Jacobian matrix is just $\frac{\partial \dot{u}}{\partial u}$. If the parameter b is chosen to be equal to the value of u at the absolute minimum of the u -nullcline then

$\tau = 0$, which means that the eigenvalues have no real part just as in the Andronov-Hopf bifurcation. In that case we have $b = \frac{1+a-\sqrt{1-a+a^2}}{3} = 0.315$ and by setting $b = 0.316$ we get $\tau > 0$. Now the real part of the eigenvalues is positive and a low amplitude limit cycle (subthreshold oscillation) appears.

4.2 Time scale of subthreshold oscillations

By means of the function $g(x)$ we are able to make the duration of spikes shorter than the period of the subthreshold oscillations. This is the desired case when studying the influence of subthreshold oscillations on spike generation in a neural network. In order to choose the values of k_1 and k_2 we derive an approximate expression for the excitation and refractory intervals looking at the slow motion equation of the u-nullcline $v = u(u - a)(1 - u)$. We will set the excitation interval as the time spent going from point A to point B represented in Fig. 9, which can be obtained by integrating the equation (25) between v_A and v_B using as a first approximation, $u(t) \approx 1$.

$$v_A = v \left(\frac{1}{3} \left[(1 + a) - (1 - a + a^2)^{1/2} \right] \right), \quad (29)$$

$$v_B = v \left(\frac{1}{3} \left[(1 + a) + (1 - a + a^2)^{1/2} \right] \right) \quad (30)$$

The same thing is done for the refractory period between point C and point D using $u(t) \approx 0$. The final results are the following expressions:

$$T_{exc} = \frac{4(1 - a + a^2)^{3/2}}{27g(1 - b)}, \quad (31)$$

$$T_{ref} = -\frac{4(1 - a + a^2)^{3/2}}{27g(-b)} \quad (32)$$

The duration of a spike will be $T_{exc} + T_{ref}$.

We can also get an expression for the period of the subthreshold oscillations and numerically compare both times. We have chosen a value of b which approaches the equilibrium point to the Andronov-Hopf bifurcation ($\tau = 0$ and $\Delta = 1/\epsilon$). From equation (11) we see that the solution to the linear system

$$\frac{d}{dt} \begin{pmatrix} \bar{u} \\ \bar{v} \end{pmatrix} = \begin{pmatrix} 0 & -1/\epsilon \\ 1 & 0 \end{pmatrix} \begin{pmatrix} \bar{u} \\ \bar{v} \end{pmatrix} \quad (33)$$

with $\lambda_{1,2} = \pm i\sqrt{\Delta}$, is an harmonic oscillator with $\omega = \sqrt{\Delta} = 1/\sqrt{\epsilon}$. The

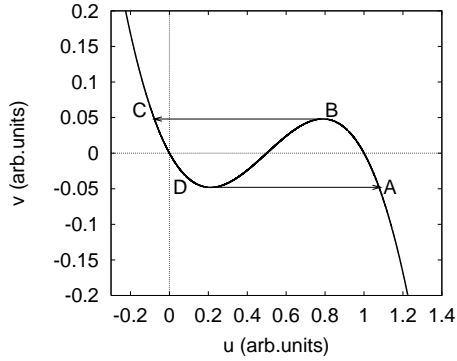


Figure 9: v -nullcline for $a = 0.5$

period of subthreshold oscillations near the bifurcation point is then $T_{sth} \approx 2\pi\sqrt{\epsilon} \approx 0.44$.

In what follows we choose $k_1 = 7.0$ and $k_2 = 0.08$ [8]. The excitation and refractory period are then $T_{exc} \approx T_{ref} \approx 0.04$, what makes the duration of a spike shorter than the period of subthreshold oscillations, T_{sth} . As shown in Fig. 10, the amplitude and duration of subthreshold oscillations is considerably increased with respect to Fig. 5. Both aspects are necessary in order to see clearly the minima and maxima of the subthreshold potential and to easily control the effect of these oscillations on the postsynaptic response and the effect of the model parameters on the oscillations.

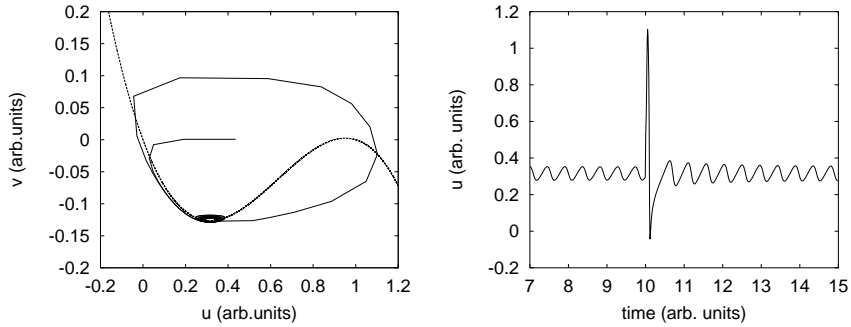


Figure 10: Phase portrait for a neuron (left) and its membrane potential time evolution (right) for the deterministic system of equations (24) and (25).

5 Spike propagation in coupled neurons

The simplest case of neural network is the coupling between two neurons. This is the basic unit of neural connection and can indeed clarify the role of subthreshold oscillations in the mechanism of spike propagation. The aim of this section is to bring insight into the modulation of information transmission in neural networks.

In what follows we will work with the model presented in Sec. 4, adding the corresponding terms for the electrical and chemical coupling introduced in Sec. 3. The values of the coupling parameters that we will use are specified in Table 1, and an example of the dynamical behavior of $C(t)$ and $r(t)$ is represented in Fig. 11. We also add an external current to the presynaptic voltage variable equation consisting on a train of pulses of 2 units of amplitude with a period of 10 units of time.

Parameter	Synapses
α	2.0
β	1.0
C_{max}	1.0
g^{syn}	(specified in each case)
τ_{syn}	0.006
τ	(specified in each case)
E_s	0.7

Table 1: Parameter values of the coupling models used in this work.

5.1 Electrical coupling: resynchronization *versus* damping

Synchronization of subthreshold activity takes place only via gap junctions. Fig. 12 shows the time evolution of the membrane potential u_i of the two neurons for increasing values of the electrical coupling strength g^{elec} and in the absence of chemical coupling ($g^{\text{chem}} = 0$). For small enough g^{elec} , a spike in the presynaptic neuron (represented by a solid line in the figure) due to the external current does not excite a spike in the postsynaptic neuron (dashed line), but perturbs sufficiently the dynamics of both neurons such that synchronization of their subthreshold activity is temporarily lost [Fig. 12(a)]. The resynchronization time decreases as g^{elec} is increased [Fig. 12(b)]. For larger strengths of the electrical coupling, the subthreshold oscillations become heavily damped [Fig. 12(c)], and eventually the postsynaptic neuron pulses as a response to the presynaptic one [Fig. 12(d)]. For an intermediate level of electrical coupling [Fig. 12(b)], the resynchronization time is relatively small, the subthreshold oscillations are not heavily

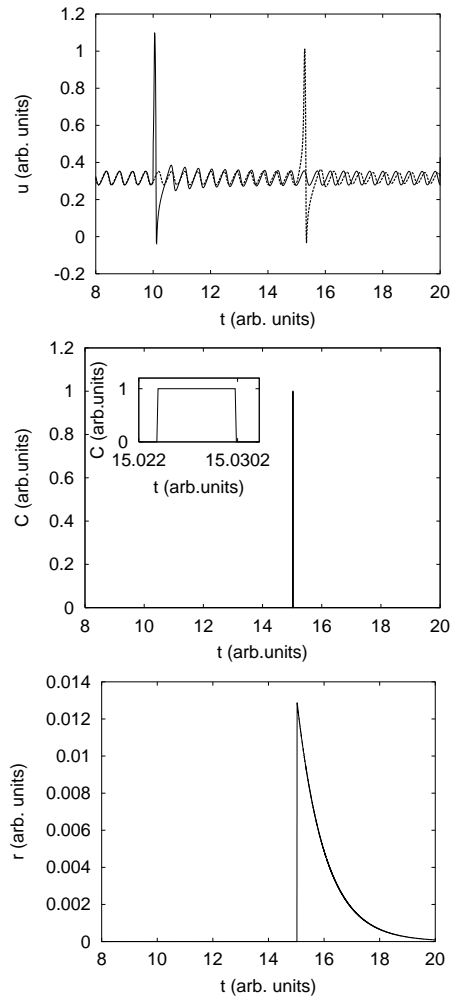


Figure 11: Time traces for two coupled neurons in the absence of electrical coupling and for $g^{chem} = 0.5$ with $\tau = 5$. The middle and bottom time traces show the dynamical behavior of C and r respectively. The solid line represents the presynaptic neuron and the dashed line the postsynaptic neuron.

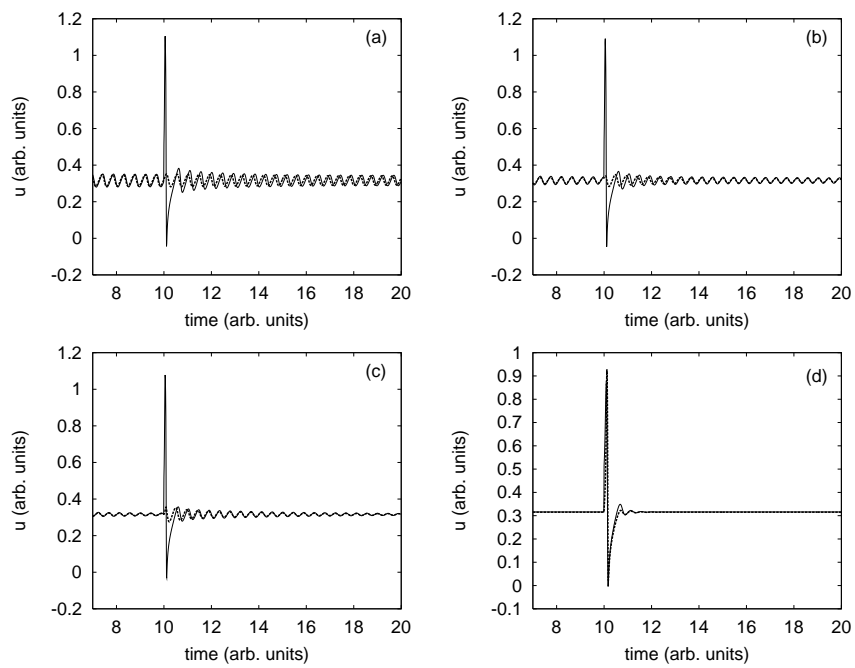


Figure 12: Time traces for the two coupled neurons in the absence of chemical coupling and for increasing strength of the electrical coupling: (a) $g^{elec} = 0.001$, (b) $g^{elec} = 0.005$, (c) $g^{elec} = 0.01$, (d) $g^{elec} = 0.1$.

damped, and the postsynaptic neuron does not pulse as a response to the presynaptic one. We will use $g^{elec} = 0.005$ in what follows.

5.2 Chemical coupling: modulating spike excitation *via* subthreshold oscillations

As mentioned above, chemical coupling is only able to propagate suprathreshold activity. If g^{chem} is too high the postsynaptic neuron will fire whenever the presynaptic neuron does, and if its too low it will never fire. In both such cases, the subthreshold activity of the postsynaptic neuron does not play a relevant role. For intermediate values of g^{chem} , on the other hand, the receiving neuron will fire depending on its state at the time at which the input pulse from the previous neuron is received. In Fig. 13 we examined the behavior of the neurons for different values of g^{chem} in the absence of electrical coupling ($g^{elec} = 0$) in order to determine whether subthreshold oscillations have an effect on the propagation of a spike. From that figure,

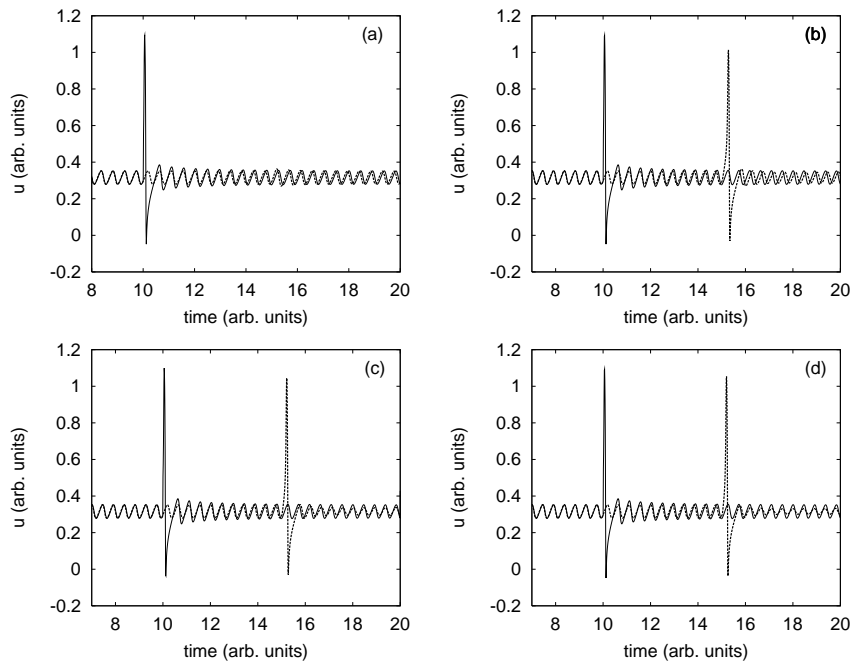


Figure 13: Time traces for the two coupled neurons in the absence of electrical coupling and for increasing strength of the chemical coupling. A delay $\tau = 5$ is externally added in order to clearly separate the spikes of the two neurons. (a) $g^{chem} = 0.1$, (b) $g^{chem} = 0.5$, (c) $g^{chem} = 0.8$, (d) $g^{chem} = 1.0$.

however, we cannot make a choice of the value of g^{chem} . We cannot yet distinguish the reason of the success or failure of the propagation of the spike of

the presynaptic neuron because we cannot predict if this will change when introducing the electrical coupling or as we vary the delay. Fig. 13(a) shows the case of a low value of g^{chem} , for which the second neuron does not fire. Varying the delay τ we see that the postsynaptic neuron never fires irrespective of the instant at which the pulse from the first neuron is received with respect to the subthreshold oscillation state (results shown in next subsection in Fig. 14(a)). For higher coupling strength g^{chem} [Fig. 13(b), (c) and (d)], on the other hand, the receiving neuron fires in response to the emitting one for the case presented in the figure, while it does not fire for other delay values (results shown in next subsection in Fig. 14(b), (c) and (d)).

5.3 Effect of delay in synaptic transmission

As mentioned in the previous section, it turns out that $g^{chem} = 0.1$ is too small and the spike of the presynaptic neuron does not propagate for any value of the delay [Fig. 14(a)]. For larger values of g^{chem} , as suggested above in the case of no electrical coupling, spike transmission depends on the delay [Fig. 14(b), (c) and (d)]. We now wish to compare the behavior of the two coupled neurons for different values of the delay introduced in the chemical current, in the presence of both synaptic and electrical coupling. To that end, we vary the delay and check the behavior of the receiving neuron for the values of g^{chem} chosen before.

Different results appear in the presence of the electrical current and given g^{elec} the postsynaptic neuron does not fire at the same values of τ that it did in the absence of the electrical current. For $g^{chem} = 0.5$ the spike doesn't propagate in the presence of electrical coupling [Fig. 15(a)] as the synchronization between the two neurons is strong enough to inhibit the excitation of the postsynaptic neuron. For $g^{chem} = 0.8$ the strength of the synchronization seems to depend on the delay introduced [Fig. 15(b)]. This observation shows the significance of the subthreshold dynamics of the postsynaptic neuron in propagating the signal in front of the persistent electrical current. We finally set $g^{chem} = 1.0$ and $g^{elec} = 0.005$, where we can look at different situations in a framework where subthreshold oscillations play a role in filtering the propagation of the signal. For example, the postsynaptic neuron can be at the maximum of its subthreshold oscillations, or at the minimum, or somewhere in between, at the moment at which it receives an external signal from the presynaptic neuron. We are interested on how the subthreshold oscillations of the postsynaptic neuron can increase the probability to propagate a spike when it is excited by the presynaptic neuron. As shown in Fig. 16, at different situations the response of the receiving neuron is different, it can either fire or not.

The results of Fig. 16 allows us to infer a non-monotonic dependence of the spike propagation efficiency on the timing at which the postsynaptic

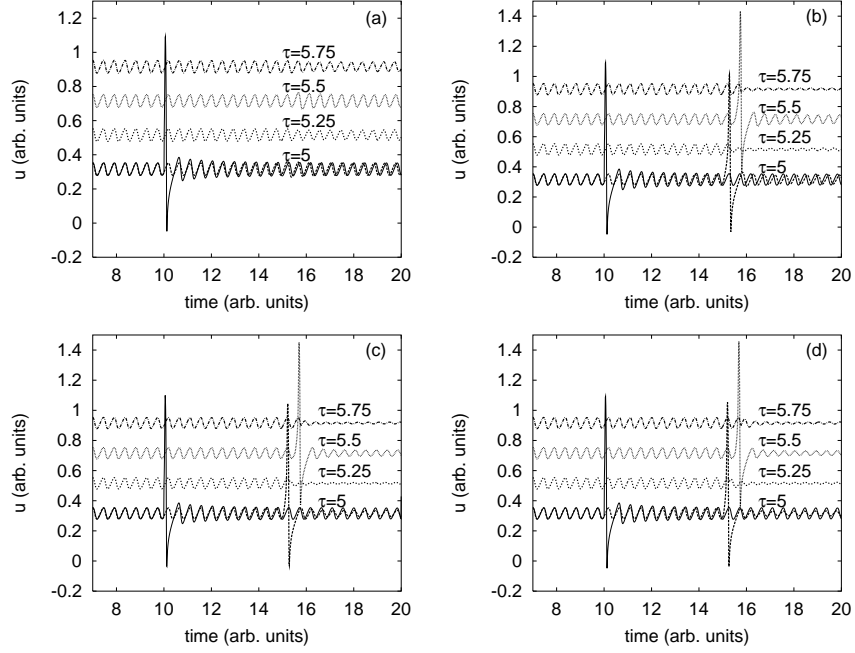


Figure 14: Time traces for the two coupled neurons in the absence of electrical coupling and for increasing strength of the chemical coupling and different values of τ . (a) $g^{chem} = 0.1$, (b) $g^{chem} = 0.5$, (c) $g^{chem} = 0.8$, (d) $g^{chem} = 1.0$.

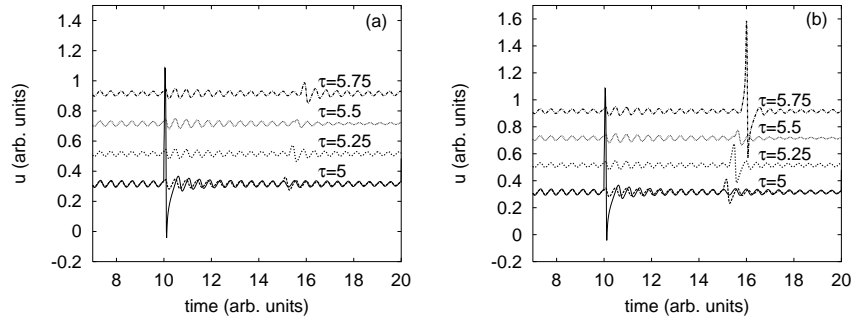


Figure 15: Time traces for the two coupled neurons with $g^{elec} = 0.005$ for different values of the delay introduced. (a) $g^{chem} = 0.5$, (b) $g^{chem} = 0.8$.

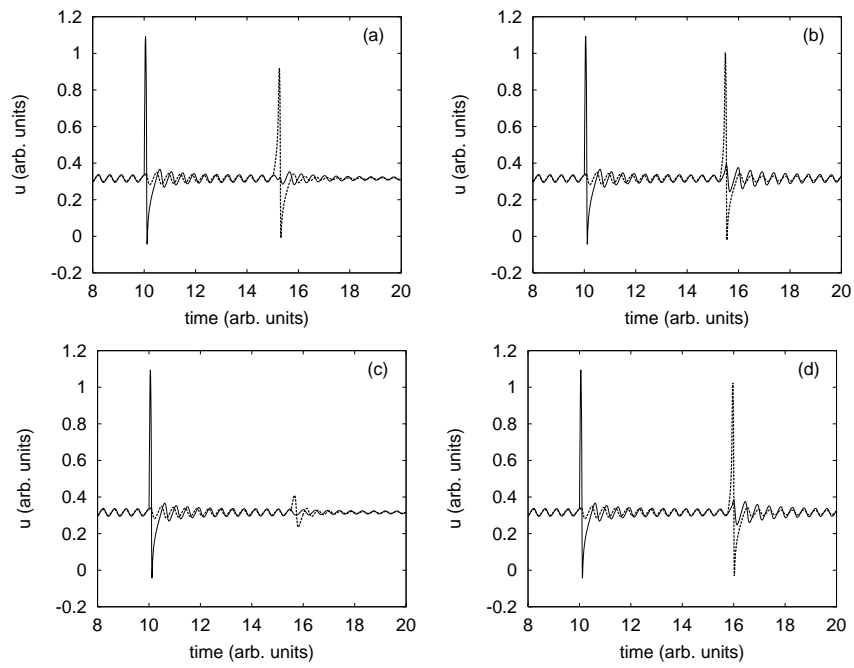


Figure 16: Time traces for the two coupled neurons with $g^{elec} = 0.005$ and $g^{chem} = 1.0$ for different values of τ . (a) $\tau = 5.0$, (b) $\tau = 5.25$, (c) $\tau = 5.5$, (d) $\tau = 5.75$.

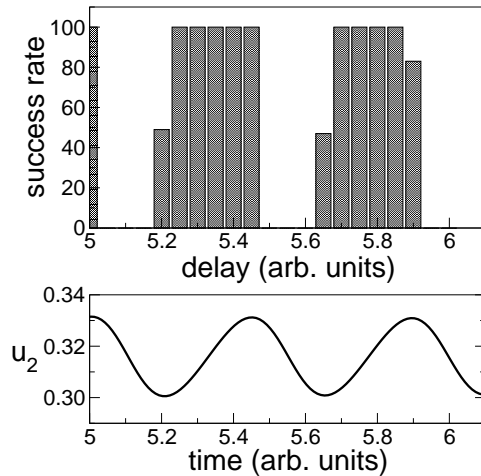


Figure 17: Success rate for increasing delay in the chemical synaptic coupling, for $g^{elec} = 0.005$ and $g^{chem} = 1.0$. The bottom time trace shows the underlying subthreshold oscillation of the postsynaptic neuron.

neuron receives the stimulus. That timing is controlled by the synaptic delay in our case, with certain delay values at which propagation is optimal and others at which is absent. In order to quantify this observation, we vary the delay from $\tau = 5$ to $\tau = 6$ in units of 0.05, stimulate the presynaptic neuron in multiple realizations (100 in the results presented here) by the external current mentioned before, and calculate the percentage of successful spike transmission events for increasing delay, [9]. As shown in Fig. 17, some delays lead to a 100% success rate, while for some others the postsynaptic neuron never fires. The figure also includes a time trace with the subthreshold oscillations that underlie the activity of the postsynaptic neuron. Comparing the top plot with the bottom time trace, one can see that the postsynaptic neuron fires when it receives the input pulse while the value of its membrane potential is growing. This can also be seen by looking carefully at Fig. 16.

6 Conclusions

We have seen that subthreshold oscillations play a relevant role in the propagation of spikes through two neurons coupled via chemical synapses. Electrical coupling via gap junctions leads to a synchronization of the background subthreshold activity, and would thus allow to scale up the phenomenon in a coherent manner to an array of coupled neurons, something which we are currently investigating. In the present case, when the membrane potential of the postsynaptic neuron is increasing the success rate of spike propagation

is at its maximum, and spike propagation is achieved. When the membrane potential is decreasing, on the other hand, the success rate drops to zero and no propagation is carried out. We expect such type of mechanism to be of general importance, given the ubiquity of gap-junction coupling and subthreshold activity in neural tissue. We have centered our work in the deterministic system even if at low values of noise intensity the subthreshold oscillations remain periodic.

References

- [1] Kandel, E.R., Scwhartz, J.H., Jessell, T.M.: *Principles of Neural Science*. 4th edn. McGraw-Hill (2000)
- [2] Llinas, R.R., Grace, A.A., Yarom, A.: *In vitro Neurons in Mammalian Cortical Layer 4 Exhibit Intrinsic Oscillatory Activity in the 10- to 50-Hz Frequency Range*. Proceedings of the National Academy of Science **88** (1991) 897-901
- [3] Giocomo, L.M., Zilli, E.A., Fransen, E., Hasselmo, M.E.: *Temporal frequency of subthreshold oscillations scales with entorhinal grid cell field spacing*. Science **315**(5819) (2007) 1719-1722
- [4] Izhikevich, E.M.: *Dynamical Systems in Neuroscience: The Geometry of Excitability and Bursting*. The MIT Press. (2005)
- [5] Verechtaguina, T., Schimansky-Geier, L., Sokolov, I.M.: *Spectra and waiting-time densities in firing resonant and nonresonant neurons* Physical Review E **70**(3) (2004) 031916-1
- [6] Balenzuela, P., Garcia-Ojalvo, J.: *Role of chemical synapses in coupled neurons with noise* Physical Review E (Statistical, Nonlinear, and Soft Matter Physics) **72**(2) (2005) 021901-7
- [7] Destexhe, A., Mainen, Z.F., Sejnowski, T.J.: *An efficient method for computing synaptic conductances based on a kinetic model of receptor binding*. Neural Comput. **6**(1) (1994) 14-18
- [8] Makarov, V.A., Nekorkin, V.I., Velarde, M.G.: *Spiking behavior in a noise-driven system combining oscillatory and excitatory properties*. Physical Review Letters **86**(15) (2001) 3431-3434
- [9] Sancristóbal, B., Sancho, J.M., Garcia-Ojalvo, J.: *Resonant spike propagation in coupled neurons with subthreshold activity*, in press in Lectures Notes in Computer Science.